

# Numerical Simulation and Analysis of Transient Current Collapse in GaN HEMTs

ChangTai Zhu, Chunlai Li, Zhijiong Wang, Jin He, Guoqing Hu, and Huayu Kang

SoC Key Laboratory, Peking University Shenzhen Institute and PKU-HKUST Shenzhen-Hong Kong Institution

## ABSTRACT

Gallium Nitride (GaN)-based high electron mobility transistors (HEMTs) are emerging as promising contenders to replace existing Silicon and Gallium Arsenide (GaAs) devices in the radio-frequency/microwave power amplifiers and high-power switching applications. In this paper, the 2-D numerical simulations of AlGaN/GaN high-electron-mobility transistor (HEMT) were carried out and analyzed to investigate the transient current collapse phenomena. The coupling between trapping effect and thermal effect were taken into account in our simulation. The turn-on pulse gate-lag transient responses with different quiescent biases were obtained, and the pulsed current-voltage (I-V) curves were extracted from the transients. The experimental results of both gate-lag transient current and pulsed I-V curves were reproduced by the simulation. These study results will help more device researchers and circuit designers understand HEMT device physics and reliability design.

**Keywords:** GaN- HEMTs, device physics, Transient simulation, current collapse, trapping effect.

## 1 INTRODUCTION

The GaN material has overall advantages comparing to the other semiconductor materials in the application area of power amplifier/switching technologies, in comparison between SiC, Si, GaAs, and InP from the basic material properties that are most important to electronic device performance [1]. As a kind of wide bandgap (WBG) material, GaN allows high electric breakdown fields and high operating temperatures. However, the advantages of these devices are limited by the radio frequency (RF) drain current collapse as well as other reliability problems [2-3]. The presence of defects is considered to be the main cause of the parasitic effects. The defects can act as trapping centers to degrade the characteristics of devices. A lot of efforts and energy have been dedicated into the investigation of trapping phenomena [4-14]. Pulsed I-V measurements are usually used to study the current collapse of GaN-based devices [3-6]. In addition, transient techniques are very useful for identification of traps in GaN HEMTs. The turn-on pulse transient tests and simulation with surface traps were carried out in [3-4]. The transient current response could not be explained with only surface donor traps, which was attributed to the interface acceptor traps [7]. The bulk trapping effect was analyzed with the transient simulation in [9-11]. Miccoli et al. contribute the gate-lag and drain-lag effects to the surface donor traps and the bulk acceptor traps, respectively [14]. However, the origin of traps is still under debate. Moreover, the traps may act as the

donor/acceptor electron/hole traps. In the previous research work, traps are supposed to be at the surface [3-4], hetero-interface [7] or in the bulk (GaN buffer layer or AlGaN barrier layer) [8-13]. Our recent work investigated the impact of bulk acceptor traps in GaN buffer on the gate-lag transient characteristics of AlGaN/GaN HEMT [15]. In this paper, based on the commercial Sentaurus TCAD software [16], the two-dimensional (2-D) numerical transient simulation work on the current collapse of Al<sub>0.3</sub>Ga<sub>0.7</sub>N/GaN HEMT in [17] is extended and discussed. By taking into account the coupling effect of traps and thermal effect, the turn-on pulse transient current responses with different quiescent biases are obtained and the corresponding current collapses are observed. The mechanism of the current collapse can be explained by the trap occupation from the view of physics. Simulation results indicate that the bulk acceptor traps can influence the gate-lag transient characteristics besides surface traps and that thermal effect may accelerate the emission of electrons for traps. Furthermore, the pulsed current-voltage (I-V) curves were extracted from the transient simulation, showing a similar current collapse trend to the experimental pulsed I-V measurement results.

## 2 STRUCTURE AND MODEL

### 2.1 Generic Structure of GaN HEMTs

The schematic cross-section structure of the device used in our simulation is shown in Fig. 1. The gate with a length  $L_g=90$  nm is in the middle between the source and drain, whereas the source-drain distance is 2  $\mu$ m. The source and drain are both Ohmic contacts with heavily doped regions. The hetero-structure is formed by a 2  $\mu$ m-thick undoped GaN buffer layer over an 18.5 nm-thick Al<sub>0.3</sub>Ga<sub>0.7</sub>N barrier layer. Moreover, a GaN cap layer with a thickness of 2 nm and a SiN passivation layer are adopted. Fig. 1. (Color online) Schematic cross-section structure of the simulated device. The Schottky barrier of the gate contact is set to 0.9 eV in the simulation. The surface donor traps with energy level  $E_d=3.0$  eV above the valence band ( $E_v$ ) and bulk acceptor traps with energy level  $E_a=0.5$  eV below the conduction band ( $E_c$ ) were taken into account in our simulation. The concentration of surface donor traps located in the interface of passivation/GaN cap layer is  $N_d=3 \times 10^{13}$  cm<sup>-2</sup>, while the bulk traps uniformly distributed in the GaN buffer have a concentration of  $N_a=5 \times 10^{16}$  cm<sup>-3</sup>. It is assumed that the electron and hole capture cross sections of the traps are  $\sigma_{n,p}=1 \times 10^{-15}$  cm<sup>2</sup>.

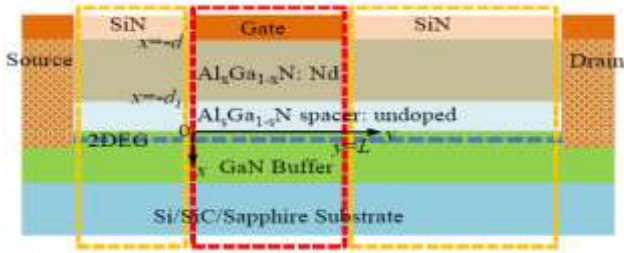


Fig.1 Cross-sectional schematic of a typical GaN HEMT.

## 2.2 Physics model

Unless specified otherwise, the parameter values for the simulation model were summarized in Table 1 and default values were used for other parameters not specified in the table. The hydrodynamic transport equations were adopted instead of drift-diffusion model to consider the role of hot electrons in the bulk trapping [11]. For thermal effect, the thermodynamic model was included with a thermal contact at the bottom of buffer, where the ambient temperature was set to 300K. Moreover, the electron mobility degradation model (i.e. HighFieldSaturation and Dopingdependence) and recombination mechanism (i.e. Shockley-Read-Hall, Auger and Radiative) were considered. Following the Sentaurus Device User Guide [16] and the work in [7, 18-19], the polarization effect was equivalent to the effect of fixed positive charges with a concentration of  $1.3 \times 10^{13} \text{ cm}^{-2}$  at the  $\text{Al}_{0.3}\text{Ga}_{0.7}\text{N}/\text{GaN}$  interface.

Table I Symbols definition in the numerical simulation. .

Parameters	Values	Units
Schottky barrier for gate	0.9	eV
Concentration of polarization charge	$1.3 \times 10^{13}$	$\text{cm}^{-2}$
Electron mobility for 2DEG/buffer	1990/1200	$\text{cm}^2/(\text{V} \cdot \text{s})$
$A_{sat}$ for saturation velocity	$2 \times 10^7$	cm/s
$B_{sat}$ for saturation velocity	$5.5 \times 10^6$	cm/s
Surface trap energy level $E_d$ from $E_v$	3.0	eV
Concentration $N_d$ of surface traps	$3 \times 10^{13}$	$\text{cm}^{-2}$
Bulk trap energy level $E_a$ from $E_v$	0.5	eV
Concentration $N_a$ of bulk traps	$5 \times 10^{16}$	$\text{cm}^{-3}$
Capture cross section $\sigma_{n,p}$	$1 \times 10^{-15}$	$\text{cm}^2$

## 3 SIMULATION RESULTS AND DISCUSSION

First, the simulated turn-on pulse gate-lag transient responses with and without thermal effect are shown in Fig. 2. A transient voltage step was applied to the gate terminal with a fixed drain bias  $V_{ds}=10 \text{ V}$ . Under this condition, the gate voltage was stepped from  $-8 \text{ V}$  (pinch-off situation for trap filling) to  $0$ . The bottom axis in Fig. 2 corresponds to the current curve with thermal effect (solid symbol), while the top axis is for the curve without thermal effect (empty symbol). As seen from Fig. 2, the transient currents rise with the increasing time until achieving to the steady-state current, showing gate-lag current collapse. Similar phenomenon was also

observed in the experimental measurement [7]. It has been proved that gate-lag current collapse can be resulted from surface donor traps [3-4]. We also reproduced this phenomenon by the simulation with only surface donor traps, where the GaN cap layer was eliminated and the negative polarization sheet charge at the interface of AlGaN barrier/passivation layer was included, proving the influence of surface traps (see Fig. 3, the surface trap energy  $E_d$  is referred to the conduction band for this simulation). However, except the result in Fig. 3, since the negative polarization charge at the interface of AlGaN barrier/GaN cap layer is not taken into account in this work, the surface trapping effect will not manifest itself according to the virtual gate theory. Therefore, the current collapses are mainly due to the bulk acceptor traps, and we have investigated the bulk trapping effect on the gate-lag transient of AlGaN/GaN HEMT[15].

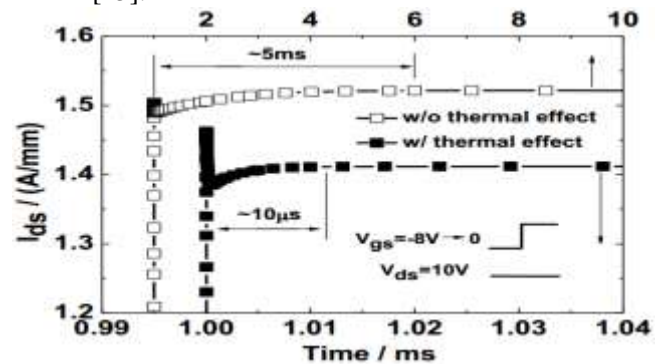


Fig. 2. Simulated turn-on pulse gate-lag transient current responses of  $\text{Al}_{0.3}\text{Ga}_{0.7}\text{N}/\text{GaN}$  HEMT with/without thermal effect.

Thermal effect exists in the practical devices and influences the electric characteristics of them. Therefore, we took the thermal effect into account in all the following simulations. The transient currents of  $\text{Al}_{0.3}\text{Ga}_{0.7}\text{N}/\text{GaN}$  HEMT with different quiescent biases are plotted in Fig. 4. In this simulation, the device was first set to the pinch-off situation with different quiescent bias points ( $V_{gsQ}$ ,  $V_{dsQ}$ ) and then was turned to the open-channel state ( $V_{gs}=0$ ,  $V_{ds}=10 \text{ V}$ ). Compared with the case of  $V_{gsQ}=0$  and  $V_{dsQ}=0$ , there is a rising trend for the current with  $V_{gsQ}=-8 \text{ V}$  and  $V_{dsQ}=10 \text{ V}$  (see Fig. 4). This can be explained from the view of physics with the bulk trapping effect in the GaN buffer. The trap occupation maps for different cases at  $t=1 \mu\text{s}$  after turning on the device are shown in Fig. 5. It is obvious that traps deep in the GaN buffer are occupied by the electrons for the second case ( $V_{gsQ}=-8 \text{ V}$ ,  $V_{dsQ}=10 \text{ V}$ ), i. e. electrons are captured by the bulk traps deep in the buffer [see Fig. 5(b)]. Therefore, the corresponding current collapse is observed. However, the captured electrons are partially emitted by the traps with the time increasing, leading to the increase of transient current (Fig. 4).

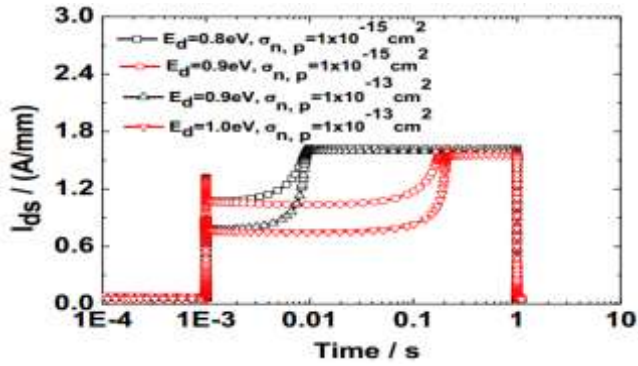


Fig. 3. (Color online) Simulation results of gate-lag transient of  $\text{Al}_{0.3}\text{Ga}_{0.7}\text{N}/\text{GaN}$  HEMT with only surface donor traps.

With the purpose of investigating the current collapse observed in the pulsed I-V measurement, the pulse transient simulation results of  $\text{Al}_{0.3}\text{Ga}_{0.7}\text{N}/\text{GaN}$  HEMT with different drain voltages are illustrated in Fig. 6. The pulsed drain voltage and the corresponding pulse transient current are shown in Fig. 6(a) and Fig. 6(b), respectively. The device is biased at  $V_{gsQ}=0$  and  $V_{dsQ}=0$  for the pinch-off state, while the gate voltage remains at 0 for the open-channel condition. The pulse width of  $2 \mu\text{s}$  and pulse period of  $10 \mu\text{s}$  are used. Based on this simulation, the pulsed I-V measurement result for studying current collapse can be reproduced, as discussed below. For comparison, the pulsed transient simulation with stress during the pinch-off situation was also carried out (Fig. 7). In this case, the device is biased at  $V_{gsQ}=-8 \text{ V}$  and  $V_{dsQ}=10 \text{ V}$  for the pinch-off situation. It can be seen from Fig. 7 that the current with  $V_{gsQ}=-8 \text{ V}$  and  $V_{dsQ}=10 \text{ V}$  is smaller than that with  $V_{gsQ}=0$  and  $V_{dsQ}=0$ . This is because that the pulse width is not long enough for the current recovering, i.e. there is not enough time for detrapping the captured electrons. If enough time is given, the final steady-state currents will achieve the same level for two cases, as shown in Fig. 4.

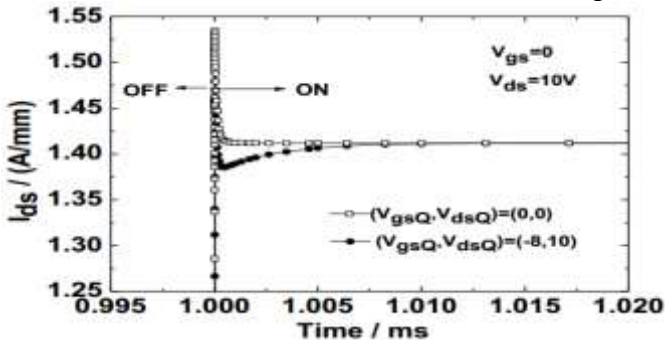


Fig. 4. Transient current curves of  $\text{Al}_{0.3}\text{Ga}_{0.7}\text{N}/\text{GaN}$  HEMT with different quiescent biases.

Furthermore, the pulsed I-V curves were extracted from the transient results with a pulse width of  $400 \text{ ns}$  and pulse period of  $10 \mu\text{s}$ . The experimental pulsed  $I_{ds}-V_{ds}$  curves of a passivated  $\text{AlGaN}/\text{GaN}$  HEMT device are given in Fig. 8(a), and the simulated corresponding characteristics of  $\text{Al}_{0.3}\text{Ga}_{0.7}\text{N}/\text{GaN}$  HEMT are illustrated

in Fig. 8(b). It is observed that current collapse can be minimized but cannot be eliminated completely by passivation due to the existence of bulk traps. Additionally, the simulation result shows the similar trend to the experimental result. Moreover, the current collapse at  $V_{ds}=4 \text{ V}$  near the knee point is larger than that at  $V_{ds}=10 \text{ V}$  for both the experimental and simulation results. In order to explain this phenomenon, the simulated transient current responses are compared between  $V_{ds}=4 \text{ V}$  and  $V_{ds}=10 \text{ V}$ , as shown in Fig. 9. The corresponding vertical electric field ( $E_y$ ) along the y direction at  $x=0.1 \mu\text{m}$  for the time  $t=1 \mu\text{s}$  is shown in the inset. As seen from Fig. 9, the current collapse at  $V_{ds}=4 \text{ V}$  is larger and the current rising time is longer than  $V_{ds}=10 \text{ V}$ . This is because that the vertical electric field at  $V_{ds}=10 \text{ V}$  is too much larger than  $V_{ds}=4 \text{ V}$  [see Fig. 9(b)], which can help the trapped electrons in the buffer coming back to the channel quickly.

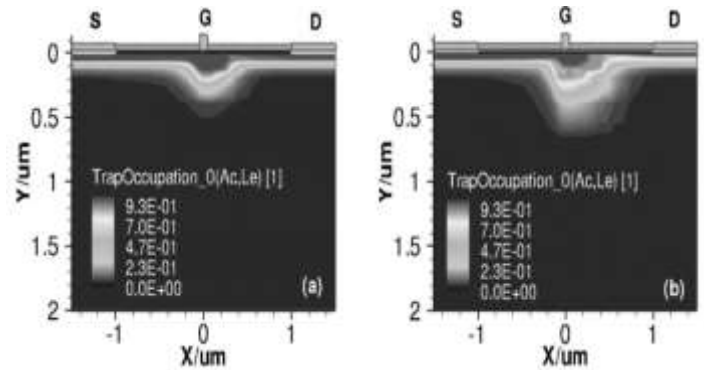


Fig. 5. Trap occupation maps at  $t=1 \mu\text{s}$  after turning on the device: (a)  $V_{gsQ}=0$ ,  $V_{dsQ}=0$ ; (b)  $V_{gsQ}=-8 \text{ V}$ ,  $V_{dsQ}=10 \text{ V}$ .

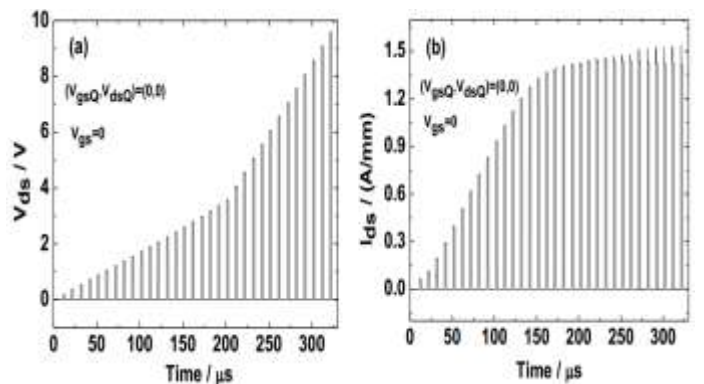


Fig. 6. Pulse transient simulation of  $\text{Al}_{0.3}\text{Ga}_{0.7}\text{N}/\text{GaN}$  HEMT with different drain voltages: (a) drain voltage; (b) drain current.



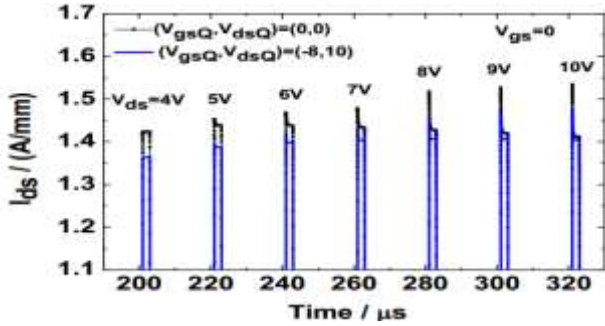


Fig. 7. (Color online) Comparison of the pulse transient currents at different quiescent biases.

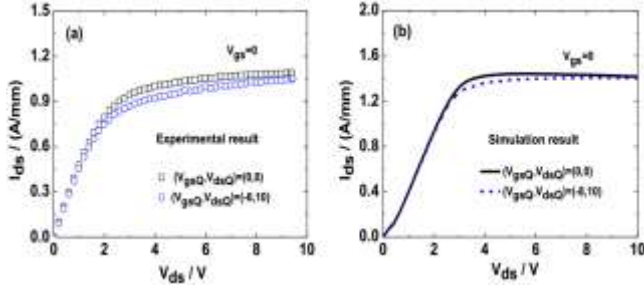


Fig. 8. (Color online) Pulsed I-V curves of GaN devices: (a) experimental results; (b) simulation results extracted from transient of  $Al_{0.3}Ga_{0.7}N/GaN$  HEMT.

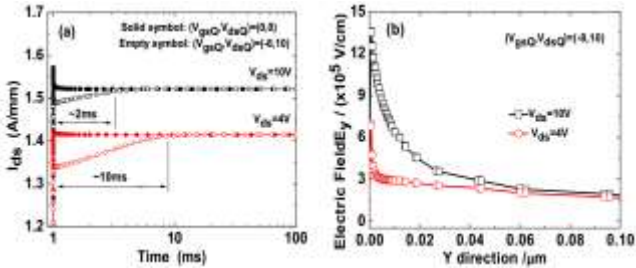


Fig. 9. (Color online) Comparison of current collapses between  $V_{ds}=4V$  and  $V_{ds}=10V$  without thermal effect: (a) transient current response; (b) the corresponding electric field  $E_y$  along the  $y$  direction at  $x=0.1\mu m$  for the time  $t=1\mu s$ .

#### 4 CONCLUSIONS

In this paper, the transient simulations of GaN HEMT were carried out and analyzed to investigate the current collapse, taking the coupling effect of trapping and thermal effect. The simulation reproduced the experimental results of both gate-lag transient current and pulsed I-V curve. In addition, simulation results indicate that bulk acceptor traps can influence the gate-lag transient characteristics besides surface traps and that thermal effect may accelerate the emission of electrons for traps. The work may help the researchers for reliability study and model development of GaN-based devices.

#### Acknowledgement

The work is funded by Fundamental Research Project of Shenzhen Sci. & Tech. Fund (JCYJ20170412153845293, JCYJ20160329161334453, JCYJ20170307164247428,

JCYJ20170307164201104, JCYJ20170307172513653, JCYJ20170412153729436, JCYJ20170412153812353), and also by Guangdong SNSFC Fund (2018A030313973).

#### References

- [1] Pengelly R S, Wood S M, Milligan J W, Sheppard S T and Pribble W L 2012 IEEE Trans. Microw. Theory Tech. 60 1764.
- [2] Klein P B, Binari S C, Ikossi-Anastasiou K, Wickenden A E, Koleske D D, Henry R L and Katzer D S 2001 Electron. Lett. 37 661.
- [3] Meneghesso G, Verzellesi G, Pierobon R, Rampazzo F, Chini A, Mishra U K, Canali C and Zanoni E 2004 IEEE Trans. Electron Devices 51 1554.
- [4] Tirado J M, Sanchez-Rojas J L and Izpura J I 2007 IEEE Trans. Electron Devices 54 410.
- [5] Yang L, Hu G Z, Hao Y, Ma X H, Quan S, Yang L Y and Jiang S G 2010 Chin. Phys. B 19 047301.
- [6] Pu Y, Pang L, Chen X J, Yuan T T, Luo W J and Liu X Y 2011 Chin. Phys. B 20 097305.
- [7] Zhang W, Zhang Y, Mao W, Ma X, Zhang J and Hao Y 2013 IEEE Electron Device Lett. 34 45.
- [8] Marso M, Wolter M, Javorka P, Kordos P and Luth H 2003 Appl. Phys. Lett. 82 633.
- [9] Braga N and Mickevicius R 2004 Appl. Phys. Lett. 85 4780.
- [10] Chini A, Lecce V D, Esposito M, Meneghesso G and Zanoni E 2009 IEEE Electron Device Lett. 30 1021.
- [11] Hu W D, Chen X S, Yin F, Zhang J B and Lu W 2009 J. Appl. Phys. 105 084502.
- [12] Meneghini M, Ronchi N, Stocco A, Meneghesso G, Mishra U K, Pei Y and Zanoni E 2011 IEEE Trans. Electron Devices 58 2996.
- [13] Bisi D, Meneghini M, Santi C, Chini A, Dammann M, Brückner P, Mikulla M, Meneghesso G and Zanoni E 2013 IEEE Trans. Electron Devices 60 3166.
- [14] Miccoli C, Martino V C, Reina S and Rinaudo S 2013 IEEE Electron Device Lett. 34 1121.
- [15] Zhou X Y, Feng Z H, Wang L, Wang Y G, Lv Y J, Dun S B and Cai S J 2014 Solid-State Electronics 100 15.
- [16] Device simulator Sentaurus TCAD Ver. D-2010.03 User's Manual, Synopsys Inc., 2010.
- [17] Zhou X Y, Feng Z H, Wang Y G, Gu G D, Song X B, and Cai S J 2014 12th IEEE International Conference on Solid-State and Integrated Circuit Technology, October 29-31, 2014, Guilin, China, accepted.
- [18] Ambacher O, Smart J, Shealy J R, Weimann N G, Chu K, Murphy M, Schaff W J and Eastman L F 1999 J. Appl. Phys. 85 3222.
- [19] Smorchkova I P, Elsass C R, Ibbetson J P, Vetury R, Heying B, Fini P, Haus E, DenBaars S P, Speck J S and Mishra U K 1999 J. Appl. Phys. 86 4520.